IMPROVING DC MOTOR SPEED CONTROL STABILITY USING PID CONTROL COMBINED WITH KALMAN FILTER IN A NOISY ENVIRONMENT

NÂNG CAO ĐỘ ỔN ĐỊNH ĐIỀU KHIỂN TỐC ĐỘ ĐỘNG CƠ DC SỬ DỤNG BỘ ĐIỀU KHIỂN PID KẾT HỢP BỘ LỌC KALMAN TRONG MÔI TRƯỜNG NHIỄU

Tan Thong Ngo[1], Minh Tu Bui Thi[2]*, Tan Cong Le[2], Nhat Truong Nguyen Tam[2]

[1]The University of Danang - University of Technology and Education, Vietnam

[2]The University of Danang - University of Science and Technology, Vietnam

*Corresponding author: btmtu@dut.udn.vn

(Received: April 06, 2026; Revised: April 29, 2026; Accepted: May 15, 2026)

DOI: 10.31130/ud-jst.2026.24(5A).229E

Abstract - This paper introduces a method to enhance DC motor speed control stability under noisy conditions. The approach integrates a conventional proportional-integral-derivative (PID) controller with a Kalman filter for feedback signal processing. The system was implemented on a microcontroller platform using two DC motors with encoders to capture real-time speed data. In practice, raw feedback signals are often corrupted by noise, causing fluctuations and reduced control performance. To address this, a Kalman filter was applied to smooth the measured signal before feeding it to the PID controller. Experimental evaluation, conducted visually via Serial Plotter and quantitatively through Excel analysis, showed that the filtered signal reduced fluctuations significantly. The standard deviation decreased by about 20% while the mean value remained nearly unchanged. These results confirm that integrating a Kalman filter with a PID controller effectively suppresses noise without distorting the measured signal, thereby improving the stability of DC motor speed control systems.

Key words - PID control; Kalman filter; DC motors; speed control; electromagnetic noise

Tóm tắt – Bài báo này trình bày phương pháp cải thiện độ ổn định điều khiển tốc độ động cơ DC trong môi trường nhiễu. Giải pháp kết hợp bộ điều khiển PID truyền thống với bộ lọc Kalman để xử lý tín hiệu phản hồi. Hệ thống được triển khai trên vi điều khiển, sử dụng hai động cơ DC gắn encoder nhằm thu thập dữ liệu tốc độ theo thời gian thực. Trong thực tế, tín hiệu phản hồi thường bị nhiễu gây dao động, làm giảm hiệu suất điều khiển. Để khắc phục, bộ lọc Kalman được áp dụng nhằm làm trơn tín hiệu đo trước khi đưa vào PID. Thí nghiệm được đánh giá qua Serial Plotter và phân tích bằng Excel cho thấy tín hiệu sau lọc giảm đáng kể dao động. Độ lệch chuẩn giảm khoảng 20% trong khi giá trị trung bình gần như giữ nguyên. Kết quả chứng minh rằng việc tích hợp Kalman với PID giúp triệt tiêu nhiễu hiệu quả mà không làm sai lệch tín hiệu đo, từ đó cải thiện độ ổn định hệ thống điều khiển tốc độ động cơ DC.

Từ khóa – Điều khiển PID; bộ lọc Kalman; động cơ DC; điều khiển tốc độ; nhiễu điện từ.

1. Introduction

Multi-DC motor control systems are widely applied in industrial automation, robotics, and electric transportation [1]; however, ensuring stable speed control under noisy conditions remains a challenging task [2]. Among available strategies, the PID controller is the most commonly adopted solution due to its simple structure and proven effectiveness [3], [4]. Nevertheless, in practice, encoder signals are frequently contaminated by electromagnetic interference (EMI) from power drivers, mechanical vibrations, and supply disturbances [2], [5], leading to degraded control performance and reduced system robustness.To improve the reliability of the feedback signal, filtering and estimation techniques have been extensively investigated. In particular, the Kalman filter has been widely acknowledged as an effective optimal estimator for dynamic systems subject to random noise [6], [7]. Previous studies have shown that incorporating the Kalman filter into PID-based DC motor control systems can significantly improve measurement quality and enhance overall control performance [8], [9], [10].

Based on this background, this paper presents a speed control system for two 24 V DC motors 72W using a PID controller integrated with a Kalman filter on an Arduino Mega 2560 platform. Speed feedback is obtained in real time from encoders with a resolution of 330 pulses per revolution. The main objective of this work is to reduce the effect of measurement noise on the feedback signal and to improve the stability and performance of the overall DC motor speed control system, (Figure 1).

The overall system architecture is illustrated in Figure 1, which depicts the hardware configuration and the signal-processing flow from measurement and filtering to control. This design enables real-time control with a short sampling period while ensuring flexibility and scalability for future multi-DC motor control applications.

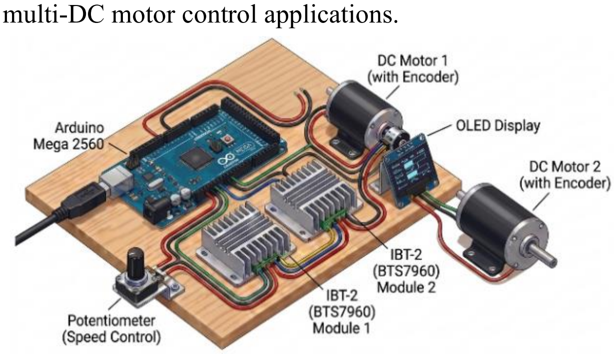

***Figure 1.** 3D diagram of the proposed experimental system*

2. System control basis and interference analysis

2.1. System Architecture and Operating Principles

The proposed DC motors speed control system operates based on a closed-loop control principle, in which the feedback signal acquired from the encoder is processed by a Kalman filter before being supplied to the PID controller. As shown in Figure 2, the system architecture consists of several functional blocks, including setpoint generation, measurement, signal filtering, control, and actuation. The speed reference is adjusted through a potentiometer and converted by the Arduino's analog-to-digital converter (ADC). The encoder signal is sampled at a period of 20 ms, providing a suitable trade-off between measurement accuracy and the processing capability of the embedded system. After Kalman filtering, both the raw and filtered speed signals are simultaneously displayed on the OLED screen, enabling real-time visual evaluation of the filter's effectiveness.

In the proposed scheme, the PID controller serves as the core component for computing the control signal from the error between the reference speed and the measured speed. This control signal is converted into a pulse-width modulation (PWM) signal and delivered to the IBT-2 power driver for DC motor actuation. The encoder generates digital pulse signals as feedback, allowing the rotational speed of the DC motor to be determined in real time.

Nevertheless, the feedback signal is frequently corrupted by disturbances such as electromagnetic interference and mechanical vibrations, which may degrade the measurement accuracy and overall control performance of the system [2], [5]. To address this issue, a Kalman filter is integrated to provide an optimal estimate of the actual DC motor speed, thereby enhancing the reliability and quality of the feedback signal [6], [7] (Figure 2).

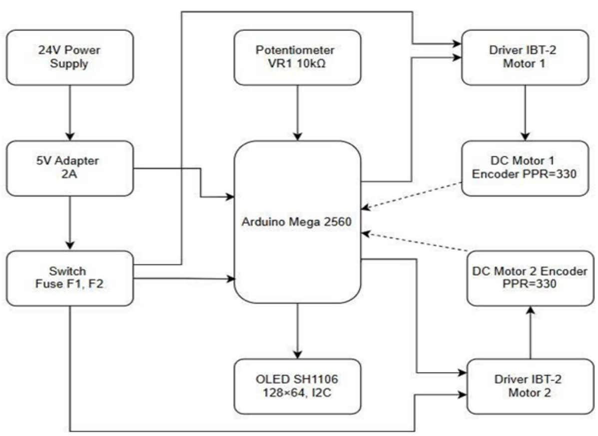

Figure 2. *Block diagram of the DC motor speed control system using a PID controller combined with a Kalman filter*

The experimental implementation of the system is illustrated in Figure 3, which includes two 24 V DC motors, two IBT-2 motor drivers, an Arduino Mega 2560 microcontroller, a potentiometer, and an OLED display (Figure 3).

In the proposed system, the Arduino Mega 2560 functions as the central processing unit responsible for executing the control and signal-filtering algorithms in real time. The microcontroller offers sufficient hardware resources to handle multiple encoder inputs simultaneously and to independently control two DC motors [11]. The IBT-2 motor driver, which is based on the BTS7960 integrated circuit, is capable of handling high current levels while providing high reliability for power-drive applications [12].

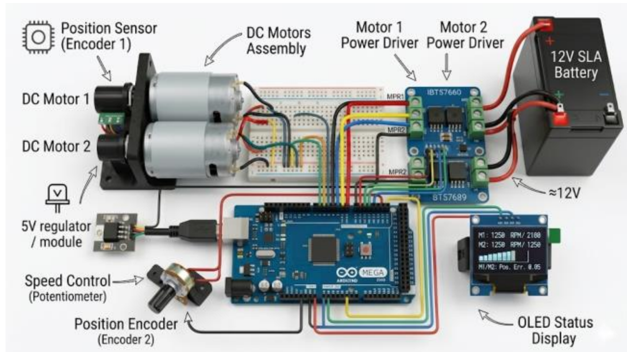

Figure 3. *Model of the dual-DC-motor speed control system*

The encoder-based speed signal is sampled at a period of 20 ms, representing a practical compromise between measurement accuracy and the computational constraints of the embedded platform. After Kalman filtering, the speed signal becomes smoother and less susceptible to noise, thereby improving the stability of PID control. The speed values before and after filtering are displayed on an OLED screen, enabling direct visual assessment of the effectiveness of the proposed approach [13].

With this control architecture, the system is able to achieve not only a rapid response but also a high level of stability under realistic noisy operating conditions. This is in agreement with recent studies on motor control in disturbed environments and multi-motor systems, in which reliability and adaptability are of critical importance [8], [14].

2.2. Control Algorithm: PID Controller and Kalman Filter

In DC motor speed control systems, the proportional–integral–derivative (PID) controller is regarded as one of the most classical control methods because of its simple structure, ease of implementation, and ability to achieve acceptable performance under a wide range of operating conditions [3], [4]. However, in practical environments, the performance of the PID controller is significantly limited by the quality of the feedback signal, especially when the system is affected by measurement noise and electromagnetic interference [2]. This issue leads to reduced stability, increased oscillations, and degraded control accuracy [5].

Considering a closed-loop control system, the error between the reference signal and the feedback signal is defined as follows:

$$e(t) = r(t) - y(t) \tag{2}$$

where $r(t)$ is the reference signal and $y(t)$ is the measured DC motor speed. The control signal of the PID controller in the time domain is expressed as:

$$u(t) = K_p e(t) + K_i \int_0^t e(\tau)\, d\tau + K_d \frac{de(t)}{dt} \tag{2}$$

where K_p, K_i, and K_d denote the proportional, integral, and derivative gains, respectively (Figure 4).

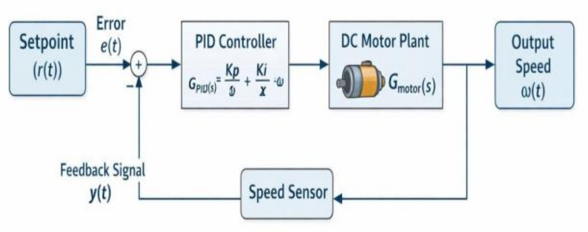

Figure 4. *Block diagram of the PID transfer function*

The transfer function of the PID controller in the Laplace domain is:

$$G_{PID}(s) = K_p + \frac{K_i}{s} + K_d s \tag{3}$$

Equation (3) can be transformed into the following rational form:

$$G_{PID}(s) = \frac{K_d s^2 + K_p s + K_i}{s} \tag{4}$$

The appropriate selection of K_p, K_i, and K_d is decisive in ensuring that the system satisfies the required performance criteria, including overshoot, settling time, and steady-state error [15]. The PID gains were initially estimated using the Ziegler–Nichols method [15] and subsequently refined empirically to achieve overshoot below 2.5% and stable response under noisy feedback. The Kalman filter parameters Q and R were determined through iterative tuning: starting from initial estimates based on encoder resolution (330 pulses/rev) and expected speed variance, Q and R were adjusted until the optimal balance between noise attenuation and phase delay was achieved. The final values Q = 0.02 and R = 10 reflect the high measurement-to-process noise ratio of the IBT-2 switching environment; the ratio Q/R = 0.002 indicates that the filter places greater confidence in the process model than in the noisy measurement. All parameter values are summarized in Table 1.

However, in practical systems, particularly those using encoders for speed measurement, the feedback signal is often corrupted by disturbances such as electromagnetic interference, quantization error, and mechanical vibration [2]. These noise components usually have a wide frequency spectrum, in which high-frequency noise severely affects the derivative term of the PID controller. Since differentiation amplifies high-frequency components, noise may be significantly magnified, resulting in oscillatory control signals and even local instability of the system [5].

Address this issue, signal-filtering techniques are employed to improve the quality of the feedback signal. Among them, the Kalman filter is considered an optimal method in the least-squares sense, allowing the system state to be estimated from noisy measurements [6]. Unlike simple linear filters, the Kalman filter utilizes the system state-space model to combine information from both the prediction model and the measurement signal, thereby providing an optimal estimate according to the mean-square error criterion.

The discrete-time state-space model of the system is described as follows:

$$x_k = Ax_{k-1} + Bu_k + w_k \tag{5}$$

$$z_k = Hx_k + v_k \tag{6}$$

where x_k is the state vector at time step k, u_k is the control input, and z_k is the measurement signal, while A, B, and H are the system matrices. The process noise w_k and measurement noise v_k are assumed to be zero-mean white Gaussian noise processes with covariance matrices Q and R, respectively [6].

The Kalman filtering algorithm consists of two stages: prediction and update. In the prediction stage, the state and the error covariance are estimated according to:

$$\hat{x}_k^- = A\hat{x}_{k-1} + Bu_k \tag{7}$$

$$P_k^- = AP_{k-1}A^T + Q \tag{8}$$

In the update stage, the Kalman gain is determined by:

$$K_k = P_k^- H^T (HP_k^- H^T + R)^{-1} \tag{9}$$

Subsequently, the state and error covariance are corrected as follows:

$$\hat{x}_k = \hat{x}_k^- + K_k(z_k - H\hat{x}_k^-) \tag{10}$$

$$P_k = (I - K_k H)P_k^- \tag{11}$$

From (7)–(11), the Kalman gain K_k is crucial in balancing confidence between model prediction and measurement. When measurement noise is high (large covariance R), the filter relies more on the model; when noise is low, the measured signal is weighted more. This allows the Kalman filter to adapt to noisy conditions and improve state estimation accuracy.

In DC motor speed control, embedding the Kalman filter into the PID loop offers clear benefits. The filtered speed signal reduces noise, limiting its impact on the derivative term of the PID controller. Consequently, oscillations are suppressed and stability improves. Studies confirm that this combination enhances performance in noisy, encoder-based systems [8], [9].

In summary, the hybrid PID–Kalman structure leverages the simplicity of PID control and the optimal estimation capability of the Kalman filter, forming the theoretical basis for the proposed system.

2.3. Hardware Configuration

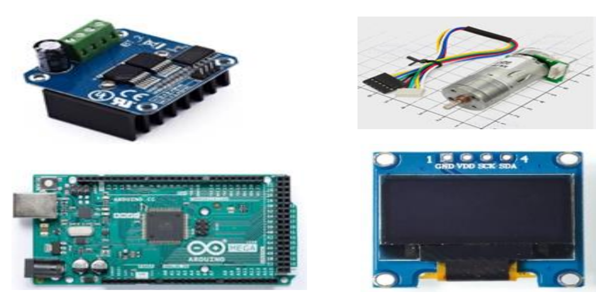

Figure 5. *Main components*

The hardware platform consists of five main components. First, the Arduino Mega 2560 (ATmega2560) serves as the central unit, handling encoder acquisition, Kalman filtering, PID computation, and PWM generation in real time [11]. Second, the IBT-2 motor driver, based on the BTS7960 IC, operates as a high-current H-bridge with built-in protections, suitable for high-power DC motors, though its switching produces EMI that can affect encoder feedback

[12]. Third, a 24 V DC motor with a 330-pulse/rev incremental encoder provides speed measurement, but the signal is sensitive to noise and vibration [2], [5]. Fourth, an OLED display (I2C) shows both measured and filtered speed in real time. Finally, a potentiometer sets the reference speed via the Arduino's ADC (Figure 5).

2.4. Hardware Implementation and PCB Design

The proposed system was designed in Altium Designer, including both the complete schematic diagram and the PCB layout. Particular emphasis was placed on noise mitigation during the hardware design process. Specifically, the encoder signal traces were physically separated from the power traces, decoupling capacitors were positioned close to the microcontroller power pins, and a continuous ground plane was employed to suppress electromagnetic interference. In addition, the DC motor supply traces were designed with sufficient width to withstand the required current, whereas the encoder signal traces were isolated to reduce crosstalk [16], [18]. After fabrication and assembly, the resulting PCB provided stable system operation and substantially reduced noise compared with conventional point-to-point wiring.

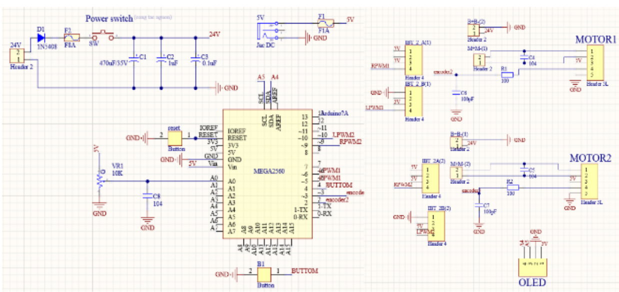

Figure 6. *Circuit diagram of the control system*

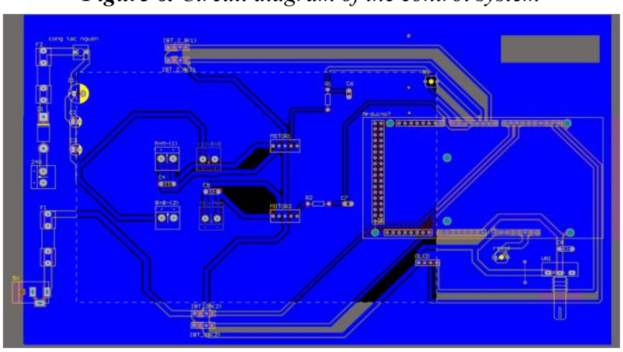

Figure 7. *PCB layout of the system*

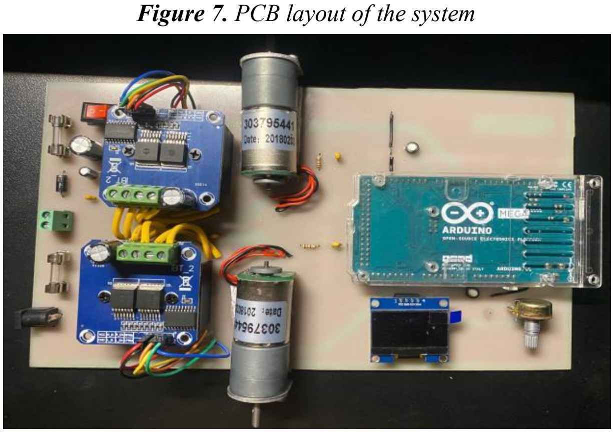

Figure 8. *Experimental prototype after fabrication*

3. Experimental Results and Evaluation

This section presents the experimental results for a comprehensive evaluation of the effectiveness of the Kalman filter in improving the speed signal quality of the two-DC-motor control system. The evaluation was conducted using two complementary approaches, namely qualitative analysis based on real-time visual observation of the signal and quantitative analysis based on the statistical characteristics of the collected data.

During the experiments, two types of speed signals were simultaneously recorded for each DC motor: (i) the raw speed signal calculated directly from the encoder, and (ii) the speed signal processed by the Kalman filter in combination with the PID controller. All data were transmitted from the microcontroller to a computer through serial communication and stored in Excel files, enabling detailed analysis and reproducibility of the results.

3.1. Raw Speed Characteristics of Two DC Motors

The first experiment investigated the characteristics of the raw speed signal obtained from the encoder in order to evaluate the inherent noise level before applying the filter. As observed in Figure 9, the speed signals of both DC motors exhibit large-amplitude random fluctuations, which are particularly pronounced during speed transition periods. These fluctuations reflect the combined effects of electromagnetic interference (EMI) from the power circuit, encoder pulse-counting errors, and shaft vibrations. It is noteworthy that, although both DC motors were operated under the same control conditions, their noise characteristics were not completely identical due to manufacturing tolerances and differences in mechanical loading conditions. The presence of high-frequency noise may severely affect the derivative component of the PID controller, resulting in oscillations in the control signal and a reduction in overall system stability (Figure 9).

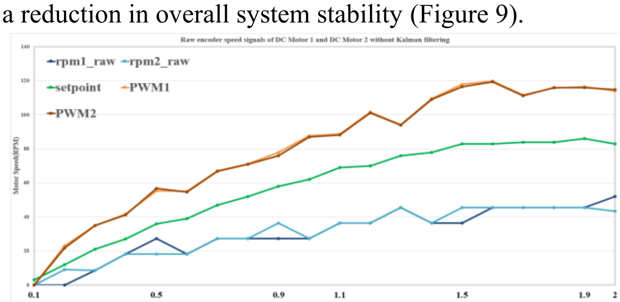

Figure 9. *Raw encoder speed signals of DC Motor 1 and DC Motor 2 without Kalman filtering*

3.2. Effect of Kalman Filtering on Speed Signals

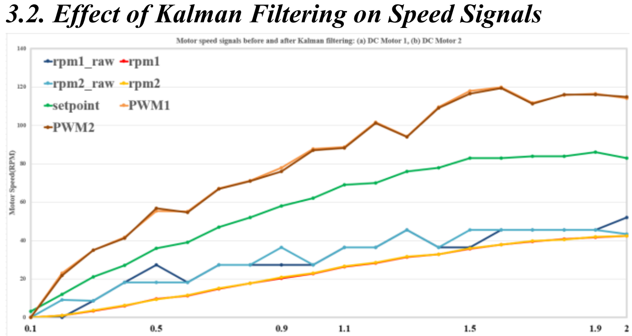

Figure 10. *Motor speed signals before and after Kalman filtering: (a) DC Motor 1, (b) DC Motor 2*

To address the limitations of the raw signal, a Kalman filter was employed to preprocess the speed signal before it was supplied to the controller. After filtering, the speed signal became noticeably smoother and more continuous, while its overall dynamic trend was well preserved, as illustrated in Figure 10. The system phase delay was estimated at ~0.04–0.06 s, corresponding to 2–3 sampling periods at Ts=0.02 s. This delay is negligible compared to the overall response time of 1.5–2 s, confirming that the Kalman filter does not introduce significant dynamic lag.

Moreover, the minimal delay highlights the filter's suitability for real-time control, as it preserves responsiveness while maintaining effective noise suppression.. More importantly, no significant increase in phase delay was observed after the introduction of the Kalman filter, indicating that the filtering process did not degrade the dynamic behavior of the system.

3.3. Quantitative Analysis from Excel Data

To provide a quantitative assessment of the effectiveness of the Kalman filter in improving the speed signal quality, the experimental data collected from the system were stored and analyzed in the Excel environment. Fundamental statistical measures, namely the mean and standard deviation, were used to characterize the signal behavior before and after filtering for both DC motors.

Table 1. *Comparison of the statistical characteristics of the speed signal*

Parameter	DC Motor 1	DC Motor 2	Unit
Proportional gain K_P	1.8	1.8	-
Integral gain K_I	0.4	0.4	-
Derivative gain K_D	0.05	0.05	-
Sampling period T_s	20	20	ms
Process noise covariance Q	0.02	0.02	-
Measurement noise covariance R	10	10	-

From Table 1, it can be observed that the mean speed values before and after Kalman filtering remain nearly unchanged for both DC motors, indicating that the filter does not distort the actual measured signal. This is an important requirement in control applications, where noise suppression must be achieved without compromising the dynamic information of the system. In contrast, the standard deviation is significantly reduced after filtering, decreasing from 14.1 to 11.3 RPM for DC Motor 1 and from 15.2 to 11.8 RPM for DC Motor 2, corresponding to reductions of approximately 19.9% and 22.4%, respectively. This reduction indicates that the filtered signal is more stable and less affected by random fluctuations.

From a statistical point of view, the decrease in standard deviation confirms that the Kalman filter effectively attenuates the noise component in the measured signal, which is consistent with the smoother signal profiles observed in Figure10. Since the Kalman filter is formulated under the assumptions of approximately linear system behavior and Gaussian-distributed noise, its performance depends on the noise characteristics of each DC motor. In the case of DC motor 2, where the noise more closely follows a Gaussian distribution, the filtering effect is more stable. By contrast, for DC motor 1, the presence of impulsive noise reduces the filter performance because the conventional Kalman filter is not specifically designed to handle outliers. Nevertheless, the results confirm that Kalman filtering significantly improves the quality of the measured speed signal for both DC motors.

Table 2. *Signal and control metrics under nominal conditions*

Metric	rpm1_raw	rpm1	rpm2_raw	rpm2	Unit
MAE	23.44	22.03	18.27	16.83	RPM
RMSE	28.40	24.92	20.10	18.27	RPM
RMSE/MAE	1.21	1.13	1.10	1.09	-
Signal fluctuation	16.52	2.63	15.87	2.51	RPM
Overshoot	-	1.98%	-	2.46%	-
Settling time (5%)	-	~7.16 s	-	~7.20 s	-

For DC Motor 1, the RMSE/MAE ratio improves from 1.21 (raw signal) to 1.13 with Kalman filtering, showing reduced average error and suppression of large spikes - critical under impulsive noise. The small overshoot (<2.5%) and settling time (~7.2 s) confirm stable PID operation with filtered feedback.

Mechanistically, when a spike occurs, the innovation residual becomes large. With high covariance R, the Kalman gain K decreases, so the estimate shifts only slightly toward the abnormal measurement, staying close to the model prediction. This explains why the Kalman filter effectively suppresses EMI-induced spikes while still tracking the true speed trend.

Table 3. *Quantitative comparison of Kalman filter performance under electromagnetic interference (EMI)*

Comparison criteria	rpm1_raw	rpm1	Unit
Standard deviation	67.72	10.34	RPM
Noise suppression factor	-	6.6×	-
Extreme spikes	-63.64 / +80.03	-	RPM
MAE with respect to the setpoint	~28.1	22.03	RPM
RMSE with respect to the setpoint	~39.8	24.92	RPM
RMSE reduction due to Kalman filtering	-	37.4%	-

The Kalman filter reduces the RMSE by 37.4% and completely eliminates extreme spike values from the feedback signal. These results confirm that the Kalman filter is a suitable choice for high-EMI environments, in which random impulsive noise is dominant. However, it should be noted that when the spike density becomes excessively high, for example, when multiple spikes occur consecutively, the Gaussian noise assumption of the Kalman filter is more severely violated, and the filtering performance may degrade. In such cases, a Robust Kalman Filter incorporating a Huber cost function would be more appropriate.

3.4. Encoder Signal Analysis at Multiple Setpoint Levels

To visually evaluate the effect of the Kalman filter on the quality of the encoder feedback signal, the quadrature encoder output signals of the two DC motors were simultaneously recorded using a two-channel oscilloscope under two conditions: without Kalman filtering and with Kalman filtering, at three setpoint levels, namely SET = 40, SET = 70, and SET = 110. Channel CH1 (yellow) corresponds to DC Motor 1, while channel CH2 (blue) corresponds to DC Motor 2. All measurements were performed in DC motors coupling mode, with a vertical scale of 2 V/div and a time base of 10 ms/div.

The results of the quadrature encoder signal analysis at the three setpoint levels under both conditions, with and without Kalman filtering, are summarized in Table 3.

The results presented in Table 4 and the oscilloscope waveforms lead to several important observations. First, the encoder pulse frequency increases proportionally with the setpoint under both conditions, confirming the linear relationship between DC motor rotational speed and encoder signal frequency, which is fully consistent with the operating principle of an incremental encoder. Second, at the same setpoint, the encoder pulse frequency in the Kalman-filtered case is consistently higher than that in the unfiltered case, with increases of approximately 100% at SET = 40; 57% at SET = 70; and 38% at SET = 110. This indicates that, by receiving a cleaner feedback signal, the PID controller is able to regulate the DC motor speed more accurately and achieve closer tracking of the reference value. The decreasing improvement trend as the setpoint increases suggests that noise has a relatively stronger effect on encoder signal quality at low speeds, whereas at higher speeds the larger pulse frequency naturally improves the signal-to-noise ratio (SNR).

Table 4. *Summary of encoder signal parameters at different setpoints*

Setpoint	Case	Channel	Fr (Hz)	+Du (%)	Rms (V)	RPM actual (OLED)
40	Without Kalman filtering	CH1-M1 (yellow)	81.7	82.4	4.36	9
40	Without Kalman filtering	CH2-M2 (blue)	81.6	75.4	4.08	10
40	With Kalman filtering	CH1-M1 (yellow)	163.3	82.4	4	35
40	With Kalman filtering	CH2-M2 (blue)	172.2	69.5	3.78	27
70	Without Kalman filtering	CH1-M1 (yellow)	152.2	82.4	4.32	27
70	Without Kalman filtering	CH2-M2 (blue)	150.7	75.1	4.05	27
70	With Kalman filtering	CH1-M1 (yellow)	238.9	82.3	4.01	45
70	With Kalman filtering	CH2-M2 (blue)	232.3	74.7	3.73	45
110	Without Kalman filtering	CH1-M1 (yellow)	240.6	82.3	4.25	45
110	Without Kalman filtering	CH2-M2 (blue)	232.3	75	4.02	36
110	With Kalman filtering	CH1-M1 (yellow)	332.2	82.3	3.98	59
110	With Kalman filtering	CH2-M2 (blue)	319.9	65.5	3.67	59

Oscilloscope results show that, without filtering, CH1 and CH2 pulse edges suffer parasitic ringing, worsening as the setpoint rises due to IBT-2 driver switching and EMI. With the Kalman filter, encoder waveforms become more stable and oscillation amplitude is reduced.

The duty cycle difference between CH1 and CH2 at the same setpoint (e.g., SET = 110: +Du = 82.3% vs. 65.5%) reflects nonuniform encoder characteristics, emphasizing the need for channel-specific Kalman tuning in multi-DC motor systems. At SET = 110, M1 Kal: 59 exceeds the raw speed M1 RPM: 54, showing the filter's ability to remove negative noise and yield a more accurate speed estimate for PID control.

Figures 11. *Encoder signals at SET = 40: (a) without Kalman filtering, (b) with Kalman filtering*

Figures 12. *Encoder signals at SET = 70: (a) without Kalman filtering, (b) with Kalman filtering*

Figures 13. *Encoder signals at SET = 110: (a) without Kalman filtering, (b) with Kalman filtering*

Overall, the quadrature encoder signal analysis obtained from the oscilloscope provides both visual and quantitative experimental evidence of the effectiveness of the Kalman filter. The results confirm that the filter not only improves the quality of the feedback signal but also significantly enhances the setpoint-tracking performance of the overall DC motor speed control system in the presence of electromagnetic interference.

3.5. Discussion

The results indicate that encoder noise reduces feedback quality, whereas the Kalman filter successfully suppresses both Gaussian and impulsive noise under all tested conditions. A sampling period of 20 ms (50 Hz) was chosen to balance accuracy with the real-time constraints of the Arduino Mega 2560, which simultaneously manages encoder acquisition, filtering, PID control, and PWM generation. Speed estimation is performed via pulse counting within each window, mitigating aliasing effects. For operating speeds of 9–59 RPM (corresponding to pulse frequencies of 50–324 Hz), system dynamics remain below 5 Hz, well within the 25 Hz Nyquist limit, thereby confirming the adequacy of the sampling rate.

The ~7.2 s settling time results from deliberately conservative PID gains ($K\_P = 1.8$, $K\_I = 0.4$, $K\_D = 0.05$), chosen to prevent overshoot under noisy feedback from the IBT-2 driver. More aggressive tuning could shorten response but risks instability; derivative filtering or anti-windup may improve robustness if required.

The 37.4% RMSE reduction also enhances hardware reliability by limiting PWM transients, thermal stress, and mechanical wear. Unlike LPF and MAF, which incur substantial delay, the Kalman filter adaptively adjusts its gain, achieving comparable noise suppression with only 0.04–0.06 s delay.

4. Conclusions

This paper presented the design and implementation of a dual-DC-motors speed control system based on a PID controller integrated with a Kalman filter on the Arduino Mega 2560 platform. Experimental results demonstrated that the Kalman filter significantly improved encoder feedback quality, reducing standard deviation by ~20% and RMSE by 37.4% under EMI conditions while preserving the mean signal value. The proposed PID–Kalman scheme confirmed stable control performance with overshoot below 2.5% and settling time of approximately 7.2 s across low, medium, and high speed ranges (SET = 40, 70, 110), with independent per-channel Kalman tuning proving essential for multi-motor systems. In future work, automatic Kalman parameter optimization, Extended Kalman Filter, and Robust Kalman Filter implementations for high-density impulsive noise environments will be investigated. In future work, automatic optimization of Kalman parameters, the application of the Extended Kalman Filter, and the implementation of a Robust Kalman Filter for environments with high-density impulsive noise may be considered.

REFERENCES

[1] F. Niu, K. Sun, S. Huang, Y. Hu, D. Liang, and Y. Fang, "A Review on Multimotor Synchronous Control Methods," *IEEE Transactions on Transportation Electrification*, vol. 9, no. 1, pp. 22–33, 2023.

[2] C. Zhang, J. Jasni, M. A. Mohd Radzi, N. Azis, and X. He, "Research and Analysis of Electromagnetic Interference of a Motor Drive Control System Based on PMSM with SiC MOSFET for New Energy Electric Vehicles," *Frontiers in Energy Research*, vol. 11, 2024.

[3] A. Ma'arif *et al*., "Control of DC Motor Using PID: Arduino Hardware Implementation," in *Proceedings of the International Conference on Industrial Engineering and Engineering (ICIEE)*, 2020, pp. 74–78.

[4] K. J. Åström and T. Hägglund, *Advanced PID Control*, ISA Press, 2006.

[5] A. J. Chan *et al.*, "A DC Motor Speed Control System with Disturbance Rejection and Noise Reduction," *IAENG International Journal of Applied Mathematics*, vol. 52, no. 4, 2022.

[6] R. E. Kalman, "A New Approach to Linear Filtering and Prediction Problems," *Journal of Basic Engineering*, vol. 82, no. 1, pp. 35–45, 1960.

[7] G. Welch and G. Bishop, "*An Introduction to the Kalman Filter,*" University of North Carolina, Technical Report TR 95-041, 2006.

[8] N. Setiawan, W. Caesarendra, and R. Majdoubi, "Implementation of Kalman Filter on PID Control System for DC Motor Under Noisy Condition," *Buletin Ilmiah Sarjana Teknik Elektro*, vol. 6, no. 3, pp. 271–280, 2024.

[9] I. D. Kurniasari and A. Ma'arif, "Implementing PID-Kalman Algorithm to Reduce Noise in DC Motor Speed Control," *International Journal of Robotics and Control Systems*, vol. 4, no. 2, pp. 958–978, 2024.

[10] S. Yuliawan *et al.*, "Kalman Filter to Improve Performance of PID Control Systems on DC Motors," *International Journal of Information Technology and Electrical Engineering (IJITEE)*, vol. 5, no. 3, 2021.

[11] Arduino, "Arduino Mega 2560 Rev3," *docs.arduino.cc,* 2023. [Online]. Available: https://docs.arduino.cc/hardware/mega-2560 [Accessed March 03, 2025]

[12] Infineon Technologies, "BTS7960 High Current PN Half Bridge NovalithIC - Datasheet, Rev. 1.1," *www.infineon.com,* 2004. [Online]. Available: https://www.infineon.com/dgdl/BTS7960_Datasheet.pdf [Accessed March 03, 2025]

[13] S. Haykin, *Communication Systems*, 5th ed., Wiley, 2009.

[14] P. Mathur and S. Raman, "Electromagnetic Interference (EMI): Measurement and Reduction Techniques," *Journal of Electronic Materials*, vol. 49, no. 5, 2020.

[15] P. M. Meshram and R. G. Kanojiya, "Tuning of PID Controller Using Ziegler-Nichols Method for DC Motor," in *Proceedings of IEEE ICAESM*, 2012, pp. 117–122.

[16] Y. Zhong *et al.*, "Mitigating Electromagnetic Interference on PCB in Electric Vehicles: A Review," *Applied and Computational Engineering*, vol. 168, no. 1, pp. 63–77, 2025.

[17] P. Q. Thai, B. T. M. Tu, N. T. Thong, N. L. C. Thanh, and T. M. Truong, "Research on Applying the H7K-A Multi-tasking Controller to a Digitally Controlled Router at the University of Da Nang," *The University of Danang - Journal of Science and Technology*, vol. 22, no. 7, pp. 12–16, 2024.

[18] P. Q. Thai *et al.*, "Estimation of the State of Lithium-Ion Battery for Electric Vehicles Using Extended Kalman Filter," in *Advances in Engineering Research and Application*, Springer, 2026, pp. 277–285.